Quantum modifications of classical diffusion in coordinate space for chaotic systems

A. R. Kolovsky, S. Miyazaki, and R. Graham
Fachbereich Physik, Gesamthochschule Essen, Universität Essen, D-45117 Essen, Germany
(Received 2 August 1993)

The paper considers the dynamics of a particle in a periodically- space- and time-dependent potential under the condition of chaos. In the classical approach the distribution function for the particle position is shown to obey a diffusion law. We study the process of diffusion in the quantum case. It is found that quantum interference effects cause an acceleration of diffusion. A charged particle in a standing-wave field is shown to be a physical system where the discussed phenomenon might be observed.

PACS number(s): 05.45.+b, 03.65.Sq, 41.75.Fr, 73.50.Yg

I. INTRODUCTION

The phenomenon of diffusion is one of the most interesting manifestations of the chaotic type of motion in classical systems. The simplest physical example of this type of diffusion is found in the model of the kicked rotor

$$H=\frac{p^2}{2}+V\cos(\theta)\sum_n\delta(t-nT) \tag{1.1}$$

described by the standard map [1]. If the initial condition for the rotor $p(0)$, $\theta(0)$ is defined with a finite accuracy $\Delta p(0)$, $\Delta\theta(0)$, the model (1.1) yields a diffusive growth of the uncertainty of the angular momentum $p(t)$; $\langle p^2(t)\rangle = V^2 t/2$.

Since the pioneering work of Chirikov and co-workers [2] the phenomenon of diffusion for the model (1.1) has been studied intensively in the quantum case, too [3]. It was found that in the quantum case, due to interference effects, the diffusion reaches saturation. It means that after some time the uncertainty of the angular momentum does not grow further. A similar modification of the diffusion process was also found in many other quantum systems like Rydberg atoms in microwave fields [4], molecules in IR fields [5], quantum Josephson junctions [6,7], atomic particle beams deflected in a standing-wave field [8], and so on. The feature common to all cited examples is a diffusion of the momentum or the energy (for the kicked rotor $E=p^2/2$). Thus the origin of all studied quantum models is the quantum kicked rotor. However, in classical mechanics there is another class of chaotic systems, which show diffusion in configuration space, and the study of these systems in the quantum case is at the very beginning [9]. A modern example of diffusion in coordinate space is ballistic electrons in a lateral superlattice [10]. In a classical approach this problem is reduced to the motion of a particle with some mass m in a periodic potential $V(x,y)$

$$H=\frac{p^2}{2m}+V(x,y),\quad V(x+a,y)=V(x,y+b)=V(x,y)\ . \tag{1.2}$$

The system (1.2) for $a=b$ was studied in detail in Ref. [11]. It was shown there that if the energy is less than $V_{\max}=\max[V(x,y)]$ the motion of the particle is generally chaotic and resembles the motion of a Brownian particle. The results of the analysis of classical systems of type (1.2) are currently used for the interpretation of experimental data for the conductivity of system electrons in a lateral superlattice in the presence of a magnetic field [12]. We note, however, that the classical approach for the system treated in Refs. [10,12] may be questioned. In fact, the value of the superlattice period a used in the experiment [10] corresponds to the scaled Planck's constant $\hbar'=1/k_F a\sim 0.1$. (k_F is the Fermi wave vector of the electrons). From previous studies of chaotic systems [3,13] we know that for such values of $\hbar'$ the quantum dynamics can differ considerably from the classical one. This gives one more reason for studying the diffusion in coordinate space in quantum mechanics.

In the present paper we propose a simple physical system, which yields diffusion in coordinate space, and study it quantum mechanically. The proposed system is a particle in the periodic potential

$$H=\frac{p^2}{2m}-V\cos(kx)\sin(\omega t)\ . \tag{1.3}$$

In the classical approach this system has properties similar to those of the system (1.2) [14] but the quantum analysis of (1.3) is easier. Besides the connection with the problem of ballistic electrons in a superlattice, the study of the system (1.3) is of interest in itself. It is shown in Sec. V that a slight modification of the model (1.3) describes the behavior of a charged particle in a standing electromagnetic plane wave. We stress that one can reduce the latter three-dimensional problem to a one-dimensional problem without approximation. From this point of view the system (1.3) is an interesting object for both theoretical and laboratory study of the process of diffusion in the quantum case.

The structure of the paper is as follows. Section II is devoted to the analysis of the classical diffusion in the system (1.3). The quantum diffusion is determined by the quasienergy spectrum (QS) and the quasienergy functions (QF) of the system, and we discuss in detail the structure of both in Sec. III. The results of the numerical simulation of the quantum diffusion are presented in Sec. IV. Section V considers the dynamics of a charged quantum

 ©1994 The American Physical Society

particle in a standing plane wave. A possible scheme of a laboratory experiment is suggested and an estimate for the required parameters of the wave is given.

II. CLASSICAL ANALYSIS

To simplify the formulas we introduce the scaled variables $x'=kx, t'=t\Omega$, $\Omega=k\sqrt{V/m}$, $\omega'=\omega/\Omega$, $p'=pk/m\Omega$, $H'=H/V$, and a scaled Planck's constant $\hbar'=\hbar k^2/m\Omega=\hbar k/\sqrt{mV}$. In the new variables the system (1.3) takes the form (primes are omitted)

$$H=\frac{p^2}{2}-\cos(x)\sin(\omega t)\ . \tag{2.1}$$

In the case of a cylindric phase space $-\infty<p<+\infty$, $-\pi<x<+\pi$ the system (2.1) is known as the double resonance model and was studied in detail in Refs. [13,15–17]. The system (2.1) shows chaotic dynamics under the condition $\omega<\sqrt{2}$. We note that the region of the chaotic motion is bounded in momentum and the shape of this region depends on time as shown in Fig. 1. If we take an ensemble of particles with the initial condition belonging to the chaotic region, then after some time and independently of the concrete form of the initial ensemble we find the particles to be uniformly distributed over the chaotic region (the so called mixing property). The time of the mixing depends on the value of the Lyapunov exponent, and for $\omega\sim 0.3$ it corresponds to 2–3 periods $T=2\pi/\omega$ of the external field.

In the case $-\infty<x<+\infty$ the chaotic region of the system (2.1) is obviously a periodic chain constructed from the "elementary" chaotic region shown in Fig. 1 (we shall further refer to it as an "elementary cell" or "cell") and every particle randomly walks along the chain. The particle moves some distance in either the positive or negative direction and is then scattered by the external alternating potential in the opposite direction. [By analogy with the model (1.2) we shall call this distance a free path.] It is convenient to measure the time in units of the period $T=2\pi/\omega$ and distance in multiples of the spatial period and, therefore, the random walk model with discrete time and discrete $x_n=2\pi n$ is most appropriate for the description of the classical diffusion.

The probability of the particle's jump from one cell to another can be determined in the following way. We uniformly distribute the particles over one cell and then, after one period T, count the number of the particles in the nearest cells. For $\omega=0.3$ we find that the probability to stay in the same cell is 0.418, the probability to jump to the next cell is 0.240; then onto the next cell the probability is 0.025; then 0.026; then less than 0.0001; and finally 0.

Figure 2 shows the evolution of the coarse-grained distribution function $F(x_n,t)$

$$F(x_n,t)=\frac{1}{2\pi}\int_{x_n-\pi}^{x_n+\pi} f(x',p,t)\,dp\,dx',\quad x_n=2\pi n \tag{2.2}$$

for the positions of the particles. The initial distribution function $f(x,p,0)$ was chosen in the form of a Gaussian packet with the center at $x=0$, $p=0$ and width $\Delta x=1/\sqrt{2}$, $\Delta p=0.1/\sqrt{2}$ (all particles belong to the center cell). The dashed line shows the results for the discrete random walk model with the transition probability as indicated above:

$$F(x_n,t+T)=0.418F(x_n,t)+0.24[F(x_{n+1},t)+F(x_{n-1},t)]+0.025[F(x_{n+2},t)+F(x_{n-2},t)]$$
$$+0.026[F(x_{n+3},t)+F(x_{n-2},t)]\ . \tag{2.3}$$

[The terms $F(x_{n\pm 4},t)$, which we omit, have a prefactor smaller than 10^{-4}.] A nice agreement is seen and, therefore, in the classical case the random walk approximation is quite good for the present problem.

We note, however, a systematic deviation from perfect diffusion which can be seen in the tails of the distribution function [the fluctuation of $F(x_n)$ is due to the statistical error]. This deviation causes the growth of the mean square $\langle x^2(t)\rangle$ to be somewhat faster than $\langle x^2\rangle\sim t$. The deviation is obviously connected with some correlations in the motion of the particle on times scales larger than one period T. The detailed study of this particular feature is not our purpose here and would require a separate paper [18].

III. STRUCTURE OF THE QUASIENERGY SPECTRUM

Now we proceed to the quantum analysis of the behavior of the coordinate uncertainty. We will assume for simplicity that the initial wave function $\psi(x,0)$ is even

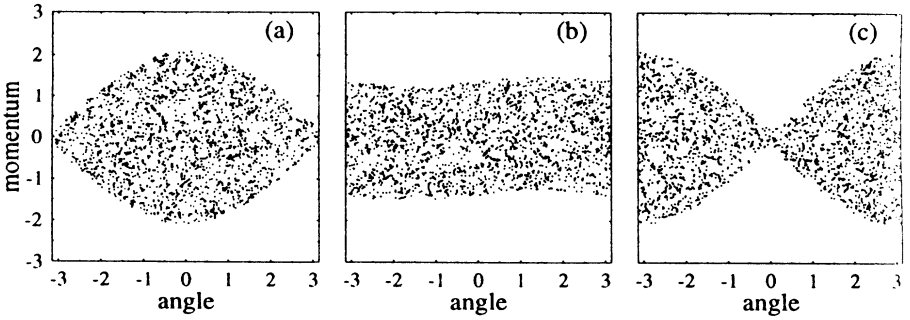

FIG. 1. The stroboscopic map of $p(t_n)$, $x(t_n)$ for the system (2.1) in the case of a cylindric phase space: $-\pi<x<\pi$, $\omega=0.3$, $T=2\pi/\omega$, (a) $t_n=Tn$, (b) $t_n=T/4+Tn$, (c) $t_n=T/2+Tn$.

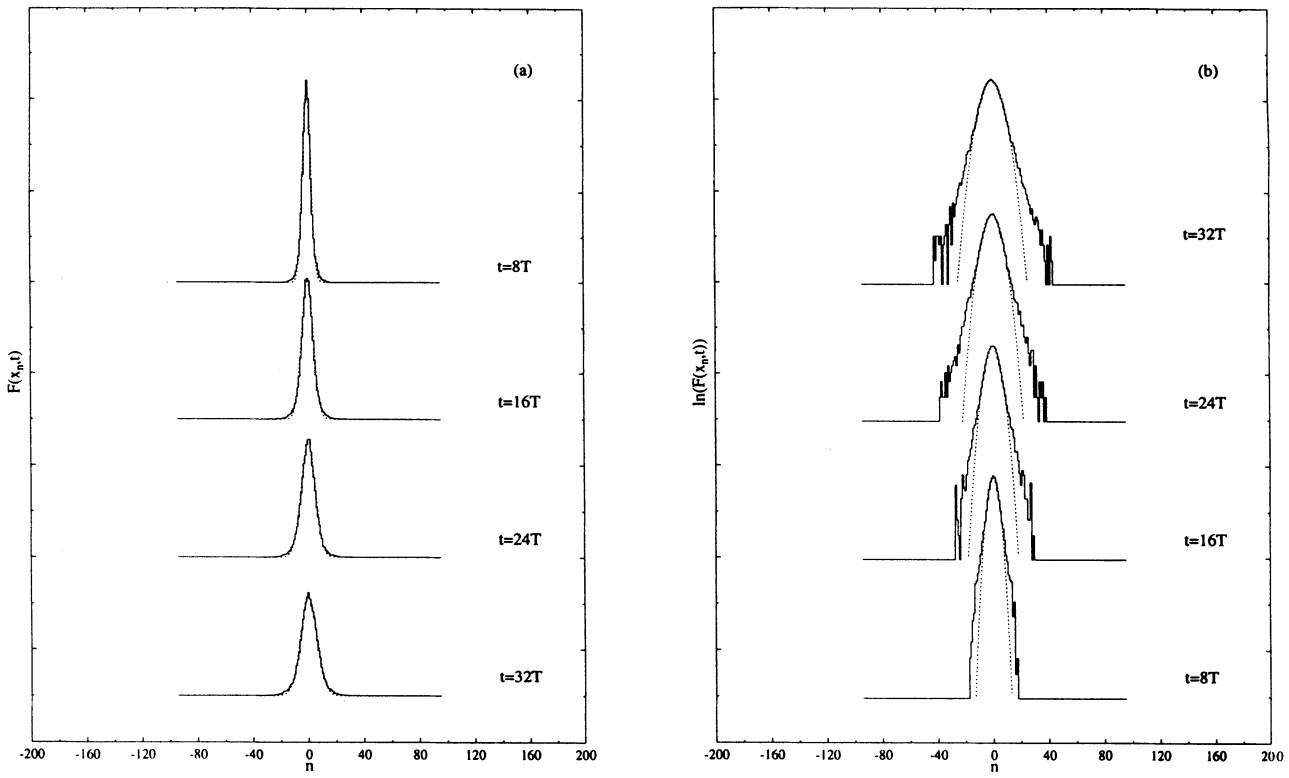

FIG. 2. Classical diffusion—the evolution of the distribution function (2.2): (a) $F(x_n,t)$, (b) $\ln[F(x_n,t)]$. The dashed lines show the results for the discrete random-walk model (2.3).

in x. In this case $\langle x(t)\rangle=0$ and the uncertainty is given by

$$\langle x^2(t)\rangle=\int_{-\infty}^{\infty}x^2|\psi(x,t)|^2dx \ . \tag{3.1}$$

Let us represent $\psi(x,0)$ in the following form:

$$\begin{aligned}\psi(x,0)&=\int_{-\infty}^{\infty}a(k)\exp(ikx)dk\\&=\int_{-1/2}^{1/2}\phi^{(k)}(x,0)\exp(ikx)dk \ ,\\ \phi^{(k)}(x,0)&=\sum_{n=-\infty}^{\infty}a(k+n)\exp(inx),\\ a(k)&=\frac{1}{2\pi}\int_{-\infty}^{\infty}\psi(x,0)\exp(-ikx)dx \ .\end{aligned} \tag{3.2}$$

Using (3.2) we can seek the solution of the problem as

$$\psi(x,t)=\int_{-1/2}^{1/2}\phi^{(k)}(x,t)\exp(ikx)dk \ , \tag{3.3}$$

where $\phi^{(k)}(x,t)$ now satisfies the Schrödinger equation with periodic boundary condition

$$\begin{aligned}&i\hbar\frac{\partial\phi^{(k)}(x,t)}{\partial t}=H^{(k)}(t)\phi^{(k)}(x,t) \ ,\\ &\phi^{(k)}(x+2\pi,t)=\phi^{(k)}(x,t) \ ,\\ &H^{(k)}(t)=\frac{\hbar^2}{2}\left[-i\frac{\partial}{\partial x}+k\right]^2-\cos(x)\cos(\omega t) \ .\end{aligned} \tag{3.4}$$

The general solution of (3.4) is the sum over the quasienergy functions

$$\begin{aligned}&\phi^{(k)}(x,t)=\sum_l b_l(k)\exp[-i\varepsilon_l(k)t]\chi_l^{(k)}(x,t) \ ,\\ &b_l(k)=\frac{1}{2\pi}\int_0^{2\pi}\phi^{(k)}(x,0)[\chi_l^{(k)}(x,0)]^*dx \ .\end{aligned} \tag{3.5}$$

Here $\chi_l^{(k)}(x,t)$ are the quasienergy functions; $\varepsilon_l(k)$ are the quasienergies in the units of $\hbar$ and by definition $0<\varepsilon_l(k)\le\omega$. Substituting (3.5) into (3.3) we finally have

$$\psi(x,t)=\sum_l\int_{-1/2}^{1/2}b_l(k)\chi_l^{(k)}(x,t)\exp\{i[kx-\varepsilon_l(k)t]\}dk \ . \tag{3.6}$$

To simplify the analysis we will consider the time t to be an integer multiple of the period T of the external potential. In this case there is no time dependence of the QF, and all time dependence is carried by the phase factors $\exp[-i\varepsilon_l(k)t]$. Therefore we should aim our efforts at the analysis of the band structure of the QS and the structure of the "static" QF which are the solution of the eigenvalue problem

$$U^{(k)}\chi_l^{(k)}(x)=\exp[-i\varepsilon_l(k)T]\chi_l^{(k)}(x) \tag{3.7}$$

for the unitary operator

$$U^{(k)}=\hat{T}\exp\left[-\frac{i}{\hbar}\int_0^T H^{(k)}(t)dt\right] \tag{3.8}$$

($\hat{T}$ denotes the time-ordering operator).

The following symmetry properties of the QS and the QF are useful to note:

$$\{\varepsilon_l(-k)\}=\{\varepsilon_l(k)\},\quad \{\chi_l^{(-k)}(x)\}=\{\chi_l^{(k)}(-x)\}\ , \tag{3.9}$$

$$\{\varepsilon_l(k+1)\}=\{\varepsilon_l(k)\},\quad \{\chi_l^{(k+1)}(x)\}=\{\chi_l^{(k)}(x)\exp(ix)\}\ . \tag{3.10}$$

From (3.9) and (3.10) we can conclude that at $k=\pm\frac{1}{2}$ the QS is doubly degenerate [19].

Equation (3.7) was solved numerically for $\hbar=0.2$. The QF's were ordered according to the quantity

$$\langle n\rangle=\sum_n n\,|c_l^{(k)}(n)|^2\ , \tag{3.11}$$

where the $c_l^{(k)}(n)$ are defined by

$$\chi_l^{(k)}(x)=\sum_n c_l^{(k)}(n)\exp(inx)\ . \tag{3.12}$$

Figure 3(a) shows the quasienergies $\varepsilon_l(k)$ corresponding to the first 21 QF's for $\omega=0.5$ [$\varepsilon_l(k)$ in the interval $(-\frac{1}{2},0)$ follows by the symmetry (3.9)]. It is seen that the behavior of the quasienergy levels $\varepsilon_l(k)$ as a function of the parameter k is as expected for a nonintegrable system and contains many avoided crossings.

To proceed further it is convenient to use the diabatic representation [20]. In the diabatic representation all avoided crossings with a gap less than some chosen $\Delta_{\max}$ are replaced by real crossings [Fig. 3(b)]. In the vicinity of a crossing the connection between quasienergies in both representations is given by the formula

$$\varepsilon_{\pm}(k)=\frac{\varepsilon_\alpha(k)-\varepsilon_\beta(k)}{2}\pm\left[\left[\frac{\varepsilon_\alpha(k)-\varepsilon_\beta(k)}{2}\right]^2+\left[\frac{\Delta}{2}\right]^2\right]^{1/2}, \tag{3.13}$$

where $\varepsilon_{\alpha,\beta}(k)$ are the quasienergies in the diabatic representation [$\varepsilon_\alpha(k)=\varepsilon_\beta(k)$ at $k=k^*$], $\varepsilon_{+,-}(k)$ are the quasienergies in the adiabatic representation, and Δ denotes the value of the gap. For the eigenfunctions of the problem the following relation is used in the diabatic representation:

$$\chi_{\pm}^{(k)}(x)=\left[\frac{1-s(k)}{2}\right]^{1/2}\chi_\alpha^{(k)}(x)\mp\left[\frac{1+s(k)}{2}\right]^{1/2}\chi_\beta^{(k)}(x)\ , \tag{3.14}$$

$$s(k)=\mathrm{sgn}(k-k^*)\left[\frac{[\varepsilon_\alpha(k)-\varepsilon_\beta(k)]^2}{[\varepsilon_\alpha(k)-\varepsilon_\beta(k)]^2+\Delta^2}\right]^{1/2}.$$

Using the diabatic picture we can "sort" all bands in two classes corresponding to states in the classically chaotic and regular regions, respectively. The first class consists of relatively narrow bands which are formed by all states associated with the chaotic component of the

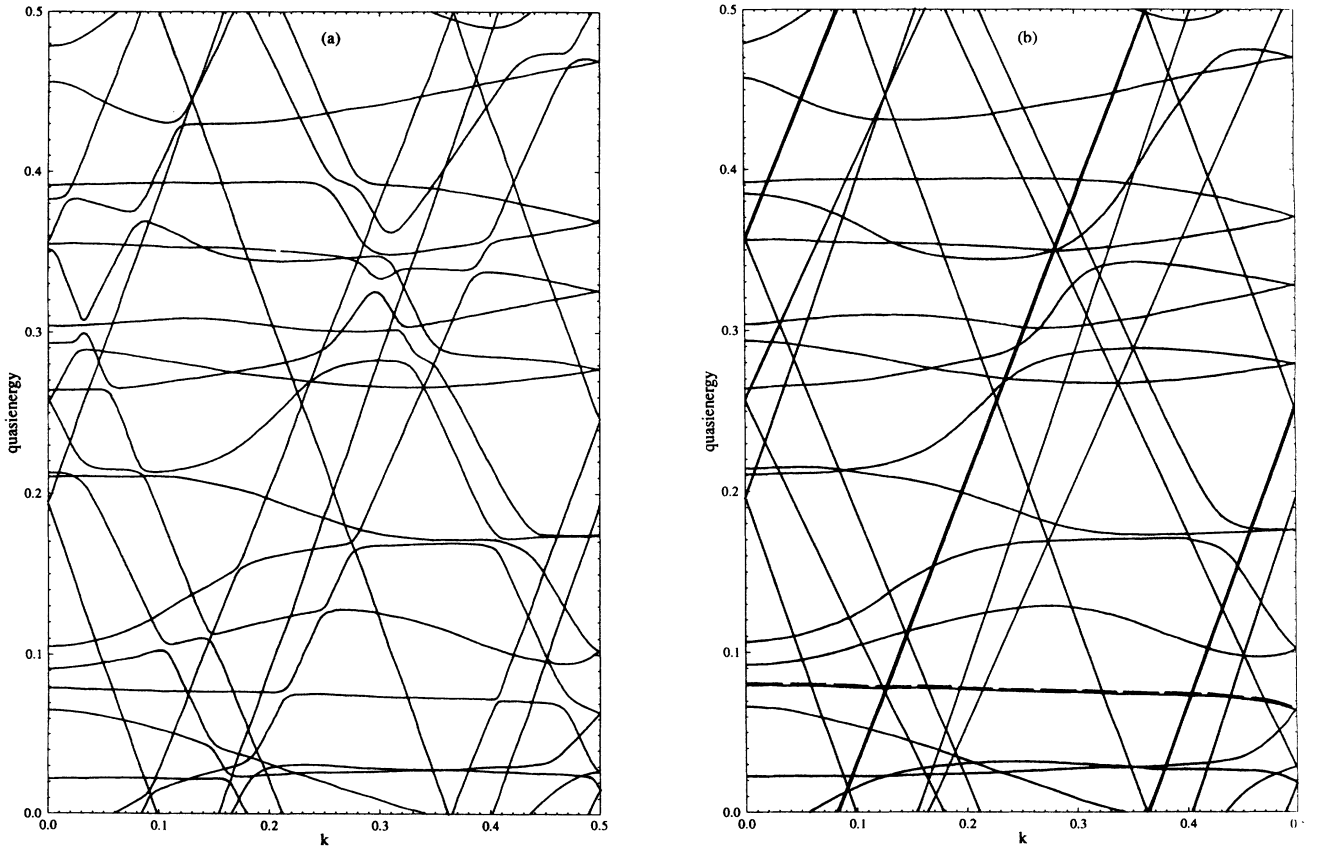

FIG. 3. (a) The band structure of the quasienergy spectrum of the quantum system (2.1) for $\omega=0.3$, $\hbar=0.2$, $0<k<\frac{1}{2}$. The quasienergies are plotted in units of $\hbar$. (b) The diabatic representation of the quasienergy spectrum. The avoided crossings with the gap $\Delta<0.01$ are replaced by real crossings.

classical counterpart (2.1) of the considered system. The Fourier expansion (3.12) of these "chaotic" QF's contains $\delta n \sim \delta I/\hbar$ (δI is the size of the chaotic region in Fig. 1) coefficients $c_l^{(k)}(n)$ which essentially differ from zero, and the quantity (3.11) is close to zero for all k. Obviously, this is the reflection of the fact that for the chaotic component the mean value of the momentum equals zero. The total number of the "chaotic" bands is also given by the parameter $\delta n = \delta I/\hbar$ and for the chosen parameter we have 15 chaotic bands.

The states associated with the regular component of the system (2.1) form the second class. They give rise to wide bands with the dispersion law

$$\varepsilon_l(k) \approx [\hbar(l+k)^2/2]_{\mathrm{mod}}\omega \approx [\hbar l k + \hbar l^2/2]_{\mathrm{mod}}\omega \ , \qquad (3.15)$$

where l is an integer and $|l| > \delta n/2$. In Fig. 3 we plot six bands of the discussed type with $l = \pm 8$, $l = \pm 9$, and $l = \pm 10$. The next QF's with $|l| > 10$ will add to the figure nearly straight lines according to the formula (3.15). The Fourier expansions of the "regular" QF's contain less than $\delta n/2$ coefficients $c_l^{(k)}(n)$ which essentially differ from zero, and "the center of gravity" $\langle n \rangle$ is placed at either negative or positive n. In the limit $|l| \to \infty$ the discussed QF's have the obvious asymptotic form $\chi_l^{(k)}(x)\exp(ikx) = \exp[i(l+k)x]$, which corresponds to the free motion of the particle with the momentum $p = \hbar(l+k)$.

If we now come back from the diabatic picture to the adiabatic one we should modify the QF's according to the formula (3.14) for the particular values of $k = k^*$ where the crossings take place. It means that for these particular values of k the "chaotic" states, which correspond to the classical motion with a finite free path, and the "regular" states, which correspond to a motion with an infinite free path, are coupled.

As an illustration of the properties of the QF's discussed above, Fig. 4 shows the absolute value of the expansion coefficients $c_l^{(k)}(n)$ for the QF's corresponding to one "chaotic" and one "regular" band marked by bold lines in Fig. 3(b). The discontinuity of the coefficients along the k axis is due to the avoided crossings. In the diabatic picture all these discontinuities are removed and the coefficients $c_l^{(k)}(n)$ are smooth functions of the parameter k.

IV. DIFFUSION IN THE QUANTUM CASE

Now we proceed to the diffusion in the quantum case. First we consider it in the diabatic picture (no avoided crossings, no coupling between the regular and chaotic states).

To consider the diffusion process we have to exclude from consideration the states which correspond to the classical motion with infinite free path. It means that the initial wave function is chosen in such a form that the expansion (3.6) contains only chaotic states. In other words, the sum over l in (3.6) is restricted to the sum over the relative narrow chaotic bands

$$\psi(x,t) = \sum_{l\,(<\delta n)} \int_{-1/2}^{1/2} b_l(k)\chi_l^{(k)}(x,t)\exp\{i[kx - \varepsilon_l(k)t]\}dk \ . \qquad (4.1)$$

In the numerical simulation we chose the initial wave function in the form of a Gaussian packet

$$\psi(x,0) = \pi^{-1/4}\exp(-x^2/2) \ . \qquad (4.2)$$

This initial state has the uncertainty $\langle \Delta x \rangle = 1/\sqrt{2}$, $\langle \Delta p \rangle = \hbar/\sqrt{2}$. Thus, for $\hbar = 0.1$, the wave packet (4.2) exactly corresponds to the initial ensemble of the classical particles used in the previous section.

Let us denote by $\Delta\varepsilon$ the characteristic width of the chaotic bands. We can consider two time limits: $t < 1/\Delta\varepsilon$ and $t \gg 1/\Delta\varepsilon$. The dynamics of the coordinate uncertainty (3.1) for these two limits is defined by different physical processes. The nonzero width of the zones is a consequence of tunneling: the quantum particle need not be scattered by the external potential even when the classical particle is. Therefore the limit $\Delta\varepsilon t \ll 1$ corresponds to the case when we can neglect the

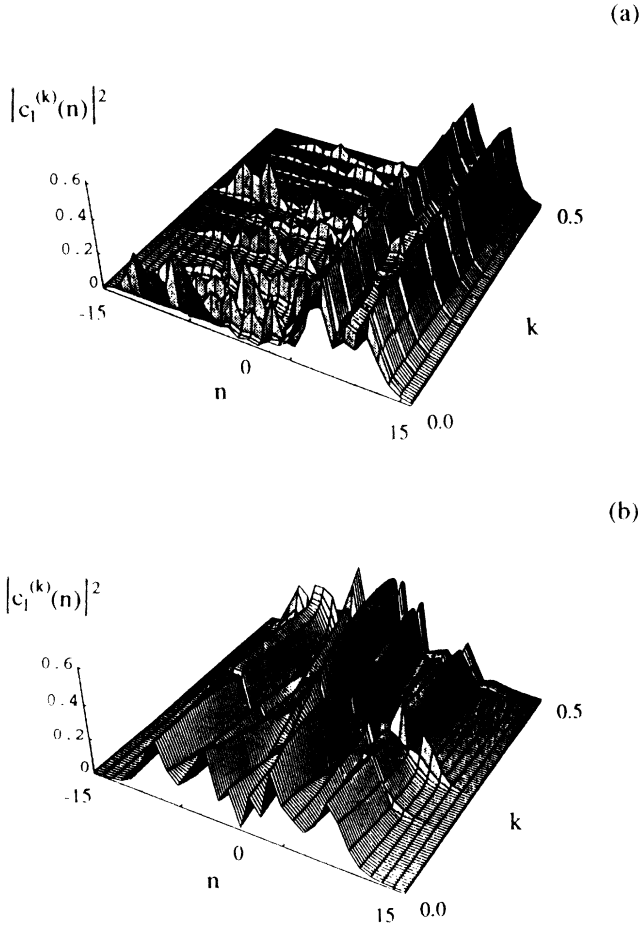

FIG. 4. The absolute values of the expansion coefficients of the quasienergy functions corresponding to the quasienergy bands marked in Fig. 3(b): (a) solid line ("regular" band), (b) dashed line ("chaotic" band). The quasienergy functions are shown in the adiabatic representation.

tunneling. In this regime the growth of the coordinate uncertainty is due to the classical scattering mechanism and the wave packet should spread as $\langle x^2(t)\rangle \simeq Dt$ where D is the coefficient of the classical diffusion.

For $\Delta\varepsilon t \gg 1$ the major role in the behavior of $\langle x^2(t)\rangle$ is played by tunneling. In this case we can estimate every term in the sum (4.1) with the help of the stationary phase method. The equation for a stationary point has the form: $d\varepsilon_l(k)/dk - x/t = 0$. While $\varepsilon_l'(k) \sim 2\pi\Delta\varepsilon$ the wave packet spreads as $\langle x^2(t)\rangle \sim (2\pi\Delta\varepsilon)^2 t^2$

Now we come back from the diabatic picture to the adiabatic one and consider the effects of the coupling of the "regular" and "chaotic" states near the avoided crossings. We note that, because of the strong dependence of the position of the avoided crossings on ω, this coupling is a resonant effect analogous to multiphoton resonance in quantum optics.

We consider a particular crossing of some chaotic band $\varepsilon_S(k)$ with some regular band $\varepsilon_R(k)$ with the dispersion law (3.15). In the adiabatic representation in the vicinity of the crossing k^* we have to replace the integral of the diabatic representation

$$\int b_S(k)\chi_S^{(k)}(x)\exp\{i[kx-\varepsilon_S(k)t]\}dk \tag{4.3}$$

in (4.1) by the integral

$$\int dk \sum_{+,-} b_\pm(k)\chi_\pm^{(k)}(x)\exp\{i[kx-\varepsilon_\pm(k)t]\} . \tag{4.4}$$

Here $\varepsilon_\pm(k)$ are given by (3.13), $\chi_\pm^{(k)}(x)$ by (3.14), and in the vicinity of k^* we have

$$\varepsilon_R(k) \approx \varepsilon_R(k^*) + \varepsilon_R'(k^*)(k-k^*) ,$$

$$\varepsilon_S(k) \approx \varepsilon_S(k^*) + \varepsilon_S'(k^*)(k-k^*) ,$$

$$|\varepsilon_S'(k^*)| \ll |\varepsilon_R'(k^*)| \approx \hbar l ,$$

$$\varepsilon_S(k^*) = \varepsilon_R(k^*) ,$$

$$b_\pm(k) = b_S(k)\left[\frac{1\mp s(k)}{2}\right]^{1/2} .$$

Thus, the coupling between the considered chaotic and regular states modifies the integral (4.3) in the vicinity of k^* in the following way:

$$\int b_S(k)\chi_S^{(k)}(x)e^{ikx}\left[\frac{1-s(k)}{2}e^{-i\varepsilon_+(k)t}+\frac{1+s(k)}{2}e^{-i\varepsilon_-(k)t}\right]dk$$
$$+\int b_S(k)\chi_R^{(k)}(x)e^{ikx}\left[\left[\frac{1-s^2(k)}{2}\right]^{1/2}e^{-i\varepsilon_+(k)t}-\left[\frac{1-s^2(k)}{2}\right]^{1/2}e^{-i\varepsilon_-(k)t}\right]dk . \tag{4.5}$$

[It is easy to see that outside the small vicinity $\Delta k \sim \Delta/\hbar l$ of k^* the formula (4.5) coincides with (4.3).] We now consider in more detail the second term in (4.5). Using the stationary phase method we can estimate it for $t \gg 1/\hbar l$ as follows:

$$\sum_{+,-} b_S(k)\exp(ilx)\left[\frac{1-s^2(k)}{2}\right]^{1/2}\left[\frac{2\pi}{t|\varepsilon_\pm''(k)|}\right]^{1/2}\exp\{i[kx-\varepsilon_\pm(k)t\pm\pi/4]\} , \tag{4.6}$$

where $k=k_\pm$ is the stationary point: $\varepsilon_\pm'(k_\pm)-x/t=0$. Because of the prefactor $\{[1-s^2(k)]/2\}^{1/2}$ the function (4.6) has a narrow maximum at $k_\pm=k^*$. For $k_\pm=k^*$ we have $\varepsilon_\pm(k^*)=\text{const}\pm\Delta/2$, $\varepsilon_\pm'(k^*)\approx\hbar l/2$, $|\varepsilon_\pm''(k^*)| \approx |\hbar l/\Delta|$. Thus, in the coordinate space the function(4.6) is a narrow peak of the height $\sim\sqrt{\Delta/t}$ which moves with a speed equal to one-half of the speed of a particle in the considered "regular" zone $\varepsilon_R(k)$. Every avoided crossing gives one peak. These peaks contribute to the t^2 law for the behavior of the squared coordinate uncertainty and because of $\hbar l \gg \Delta\varepsilon$ this contribution dominates over the contribution from the tunneling.

The results of the numerical simulation of the diffusion in the quantum case for $\omega=0.3$ are presented in Figs. 5–7. Figure 5 shows the behavior of $F(x,t)$ until $t=32T$ for $\hbar=0.1$. Figures 6(a)–6(c) shows $F(x,t)$ for $t=16T$ and different values of $\hbar$. These figures should be compared with Fig. 6(d), where the results of the classical diffusion are given. We note that Figs. 5 and 6 show the coarse-grained distribution function

$$F(x_n,t)=\frac{1}{2\pi}\int_{x_n-\pi}^{x_n+\pi}|\psi(x,t)|^2dx, \quad x_n=2\pi n . \tag{4.7}$$

The "fine" distribution function is given by the square of the wave function and it is a rapidly varying function of x. (The smaller the scaled $\hbar$, the larger the frequency of the variation, see Fig. 7.) Figures 5–7 allow us to see all effects of quantum diffusion which have been discussed above theoretically. We summarize them once more:

(a) The coupling between the "regular" and chaotic states (avoided crossings) gives rise to small peaks of the probability which propagates with constant velocity $\sim\hbar l/2$ (l is the index of the "regular" band, $|l|>\delta n/2$). These peaks contribute to the tail of the distribution function clearly seen in Fig. 7 and Figs. 6(b) and 6(c).

(b) The tunneling in configuration space (finite width of the "chaotic" bands) causes the broadening of $F(x_n)$ [see Figs. 6(b) and 6(c)]. We note that for large values of $\hbar$ it is difficult to distinguish this effect from the effect of the coupling with "regular" states [Figs. 6(a) and 6(b)]. This fact is hardly surprising because the coupling between regular and chaotic states is also caused by tunneling but in phase space rather than in configuration space.

(c) Figure 5 confirms the $\langle x^2(t)\rangle \sim t^2$ law: it is seen that the size of the domain of the support of the wave packet grows linearly in time.

The numerical simulation also shows one more interesting effect. It is clearly seen from Figs. 5 and 6 that

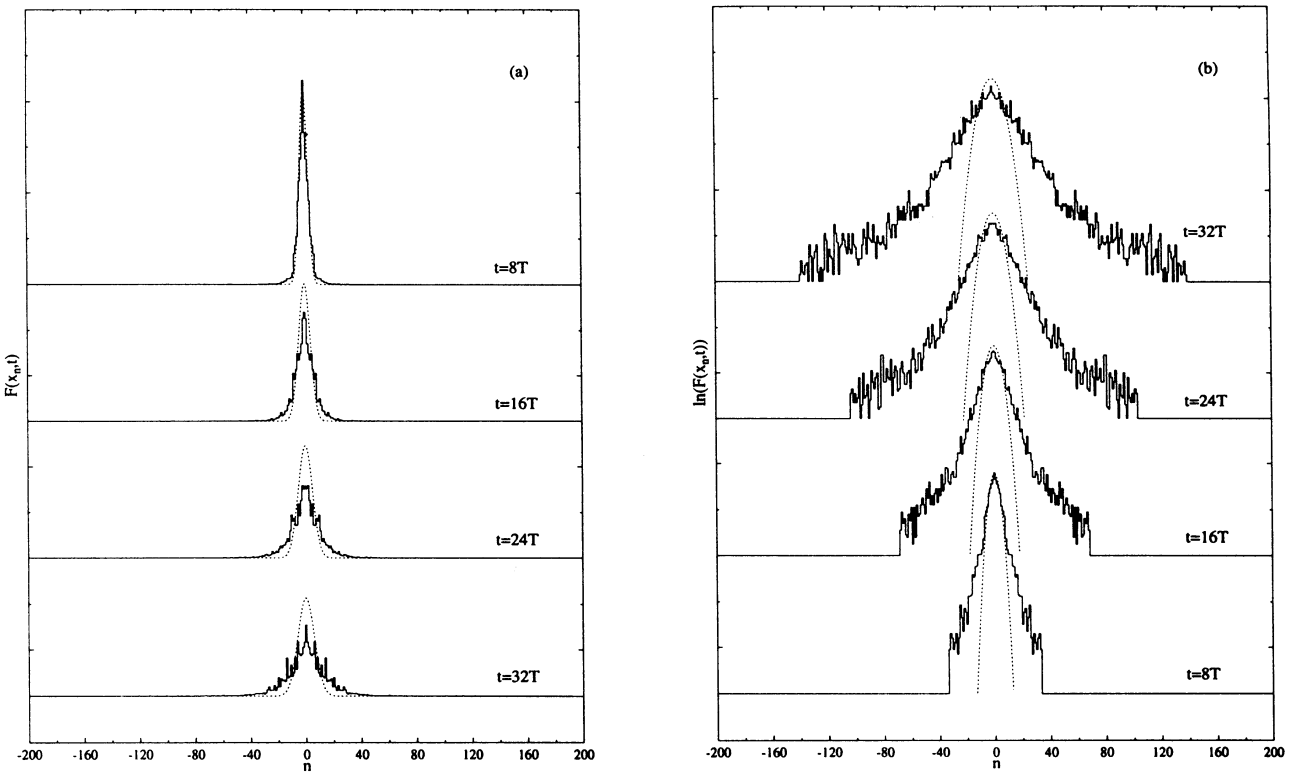

FIG. 5. Quantum diffusion—the same as for Fig. 2 but for the quantum distribution function (4.7) for $\hbar=0.1$.

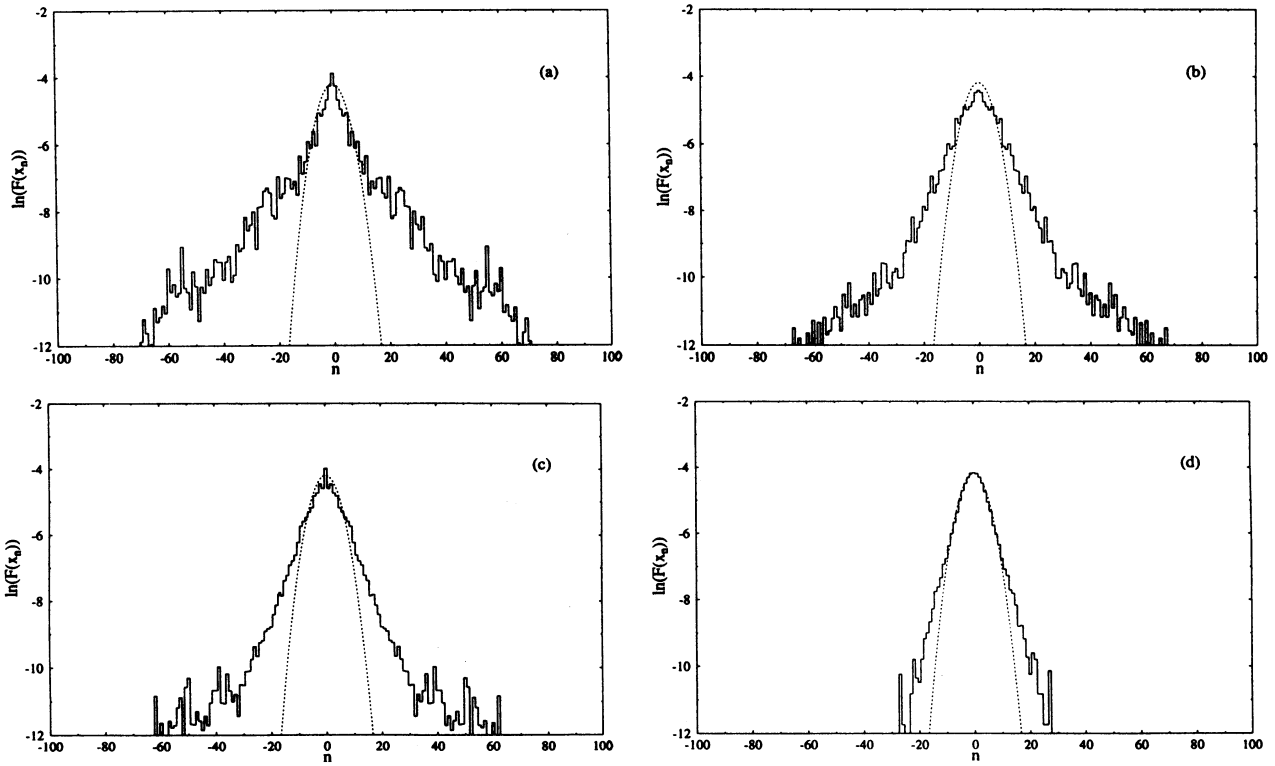

FIG. 6. The logarithm of the distribution function $F(x_n,t)$ for $t=16T$ and different values of $\hbar$: (a) $\hbar=0.2$, (b) $\hbar=0.1$, (c) $\hbar=0.04$, (d) $\hbar=0$ (classical result).

the coarse-grained distribution function $F(x_n,t)$ still shows an interference pattern. This quantum interference is very strong in the distribution function without coarse graining (see Fig. 7). However, it is quite surprising that in our case the interference pattern can "survive" after the coarse-graining procedure (4.7) even for $\hbar \sim 0.01$.

V. A CHARGED PARTICLE IN A STANDING-WAVE FIELD

The present section discusses a possible scheme of a laboratory experiment where one might be able to study the diffusion of the coordinate in the quantum case.

We consider the following system: a charged particle with the mass m and the charge q moves along the y axis and crosses vertically a standing wave with wave vector k parallel to the x axis and a polarization of the electric component parallel to the y axis. In the Coulomb gauge the vector potential $\mathbf{A}(\mathbf{r},t)=\mathbf{e}_y(Ec/\nu)\cos(kx)\cos(\nu t)$ corresponds to the given field. In the nonrelativistic case the Hamiltonian of the particle has the form

$$H=\frac{1}{2m}\left[\mathbf{P}-\frac{q}{c}\mathbf{A}(\mathbf{r},t)\right]^2 . \tag{5.1}$$

Since $\mathbf{A}$ is parallel to $\mathbf{e}_y$ the canonical momentum $P_y=mv_y+(qE/\nu)\cos(kx)\cos(\nu t)$ is an integral of the motion and, therefore, our problem reduces to the one-dimensional problem

$$H_x=\frac{P_x^2}{2m}-\frac{qEP_y}{m\nu}\cos(kx)\cos(\nu t)+\frac{E^2q^2}{2m\nu^2}\cos^2(kx)\cos^2(\nu t) . \tag{5.2}$$

From the viewpoint of nonlinear dynamics the system (5.2) is a system of three nonlinear resonances centered at $P_x=\pm mc$ and $P_x=0$. We consider the nonrelativistic case $P_x \ll mc, P_y \ll mc$ and assume that the additional condition

$$P_y \ll qE/\nu \ll mc \tag{5.3}$$

is satisfied. The condition (5.3) means that the widths of the resonances are much smaller than the distance between them and, therefore, we can consider the resonance at $P_x=0$ as isolated. In other words, with high accuracy the dynamics of the particle is described by the Hamiltonian

$$H_x=\frac{P_x^2}{2m}+\frac{E^2q^2}{4m\nu^2}\cos^2(kx) . \tag{5.4}$$

To make the motion of the particle chaotic we modulate the amplitude of the field: $E(t)=E\sin(\omega t)$ [21]. Now the system (5.4) is again a system of three nonlinear resonances and, according to Chirikov's criterion, chaos occurs for

$$\omega < (2+\sqrt{2})qE/mc . \tag{5.5}$$

We note that the condition (5.5) is a condition for the modulation frequency ω of the field amplitude (not the frequency ν of the field), and it can be easily satisfied for a particle of arbitrary mass.

For the purpose of comparison we introduce the dimensionless variables: $x'=2kx$ $t'=t\Omega$, $\Omega=qE/2mc$, $p'=2P_xk/\Omega m$, $\omega'=2\omega/\Omega$, and $\hbar'=4\hbar k^2/\Omega m = 8c\hbar k^2/qE$. (We note that $\hbar'$ does not depend on the mass of the particle.) In these variables the Hamiltonian (5.4) takes the form (primes are omitted)

$$H=p^2/2+[1+\cos(x)][1-\cos(\omega t)] . \tag{5.6}$$

Now it is seen that the system (5.6) is very similar to our model (2.1) and one can expect for it essentially the same dynamics [22].

Let us estimate the characteristic parameters of the standing wave. For electrons and an amplitude of the electric field of $E=1000$ V/cm the typical values of $\omega=0.5$ and $\hbar=0.2$ used in the numerical simulation in the previous sections correspond to a modulation frequency $2\times10^7\ \mathrm{s}^{-1}$ and a wavelength of about 0.1 mm.

A wave guide with a hole for the incoming particle and the opposite wall covered by a sensitive substance (a photopaper) may be a suitable setup. Developing the photopaper we can read the information about the coarse-

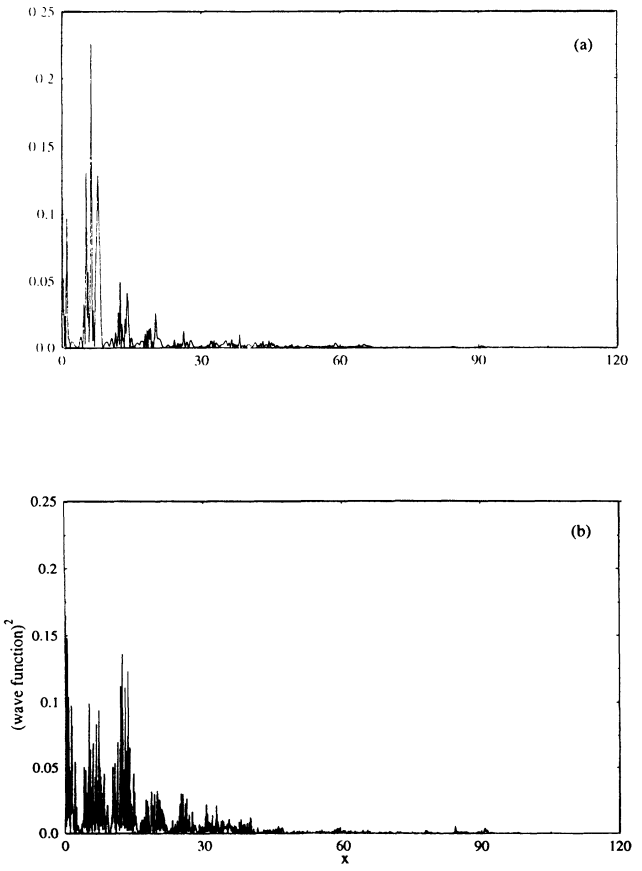

FIG. 7. Dynamics of the wave function. The figure shows $|\psi(x,t)|^2$ for $x>0$, $t=4T$: (a) $\hbar=0.2$, (b) $\hbar=0.04$. Initial wave function $\psi(x,0)=\pi^{-1/4}\exp(-x^2/2)$.

grained distribution function $F(x,t)$. The scale of the coarse graining is obviously defined by the resolution of the photopaper and it will not be a problem to reach the resolution of the order of a wavelength. (In the numerical simulation we took the resolution equal to the wavelength.) Varying the speed of the incoming particles one can vary the time t in (4.7) and, therefore, one can study "the quantum diffusion" in its dynamics.

ACKNOWLEDGMENTS

We would like to thank B. V. Chirikov and F. M. Izrailev for useful discussions. This work was performed within the Sonderforschungsbereich 237 of the Deutsche Forschungsgemeinschaft. One of us (A.R.K.) was supported by the Humboldt Stiftung, another (S.M.) by the Deutscher Akademischer Austauschdienst.

[1] A. J. Lichtenberg and M. A. Libermann, *Regular and Stochastic Dynamics* (Springer-Verlag, Berlin, 1983).

[2] G. Casati, B. V. Chirikov, F. M. Izrailev, and J. Ford, in *Stochastic Behavior in Classical and Quantum Hamiltonian Systems,* edited by G. Casati and J. Ford, Lecture Notes in Physics Vol. 90 (Springer, Berlin, 1979), p. 334.

[3] B. V. Chirikov, in *Les Houches Session LII: Chaos and Quantum Physics,* edited by M.-J. Giannoni, A. Voros, and J. Zinn-Justin (North-Holland, Amsterdam, 1991), pp. 443–546.

[4] G. Casati, B. V. Chirikov, D. L. Shepelyansky, and I. Guarneri, Phys. Rep. **154**, 77 (1987).

[5] R. Graham and M. Hohnerbach, Phys. Rev. A **43**, 3966 (1991).

[6] R. Graham, M. Schlautmann, and D. L. Shepelyansky, Phys. Rev. Lett. **67**, 255 (1991).

[7] R. Graham and J. Keymer, Phys. Rev. A **44**, 6281 (1991).

[8] R. Graham, M. Schlautmann, and P. Zoller, Phys. Rev. A **45**, R19 (1992).

[9] To our knowledge there is only one paper devoted to the outlined problem: E. Doron, U. Smilansky, and T. Dittrich, Physica B **179**, 1 (1992). The authors consider a one-dimensional chain of two-dimensional billiards and study its energy spectrum. In the classical approach this system can be considered as a chain of the chaotic scatterers and, under some conditions, diffusion along the chain may occur.

[10] D. Weiss, M. L. Roukes, A. Menschig, P. Grambow, K. V. Klitzig, and J. Weimann, Phys. Rev. Lett. **66**, 2770 (1991).

[11] T. Geisel, A. Zacherl, and G. Radons, Z. Phys. B **71**, 117 (1988).

[12] R. Fleischmann, T. Geisel, and R. Ketzmerick, Phys. Rev. Lett. **68**, 1367 (1992).

[13] G. P. Berman and A. R. Kolovsky, Usp. Fiz. Nauk. **162**, 95 (1992) [Sov. Phys. Usp. **35**, 303 (1992)].

[14] We also note a particular case where the system (1.2) can be directly reduced to our model (1.3). Let us consider a particle moving in the periodic potential $V(x,y) = V\cos(2\pi x/a)\cos(2\pi y/b)$ with energy $E \gg V$ and let $p_y \gg p_x \approx 0$. For $E \gg V$ the momentum p_y is approximately conserved $p_y = p_0 + \delta p_y(t)$, $|\delta p_y| \ll p_0$. Therefore $H \approx (p_0^2 + 2p_0\delta p_y + p_x^2)/2m + V\cos(2\pi x/a)\cos(2\pi y/b)$ and the motion in the x direction can be described with the help of (1.3) where $k = 2\pi/a$ and $\omega = 2\pi p_0/mb$.

[15] B. V. Chirikov, Phys. Rep. **52**, 263 (1979).

[16] D. F. Escande, Phys. Rep. **121**, 167 (1985).

[17] N. Moiseyev, H. J. Korsch, and B. Mirbach (unpublished).

[18] Various mechanisms of the modification of the classical diffusion are discussed in the papers of A. Zacherl, T. Geisel, J. Nierwetberg, and G. Radons, Phys. Lett. A **114**, 317 (1986); T. Geisel, A. Zacherl, and G. Radons, Z. Phys. B **71**, 117 (1988).

[19] Actually, let $\chi_l^{(-1/2)}(x)$ be the eigenfunction of $U^{(k)}$ at $k = -\frac{1}{2}$ which corresponds to the eigenvalue $\varepsilon = \varepsilon_l(-\frac{1}{2})$. According to (3.9) $\chi_l^{(-1/2)}(-x)$ is the eigenfunction of $U^{(k)}$ at $k = \frac{1}{2}$ and corresponds to the same value of ε. On the other hand, according to (3.10) the function $\chi_l^{(-1/2)}(x)\exp(ix)$ also is an eigenfunction of $U^{(1/2)}$ with the eigenvalue $\varepsilon_l(-\frac{1}{2})$.

[20] T. Takami, Phys. Rev. Lett. **68**, 3371 (1992).

[21] A similar scheme was considered in Ref. [9], but there the spatial phase of the standing wave (not its amplitude) was periodically modulated in time.

[22] A. R. Kolovsky (unpublished).

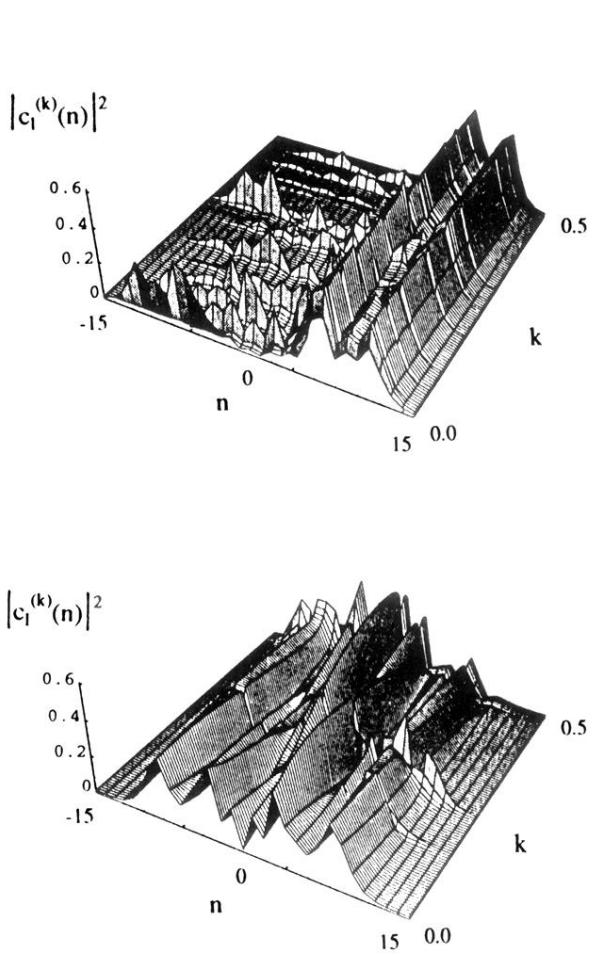

FIG. 4. The absolute values of the expansion coefficients of the quasienergy functions corresponding to the quasienergy bands marked in Fig. 3(b): (a) solid line ("regular" band), (b) dashed line ("chaotic" band). The quasienergy functions are shown in the adiabatic representation.